THE HEAVY ION BEAM PROBE

CONTENTS

PRINCIPLES OF OPERATION

A continuous beam of singly charged heavy ions, typically Tl^+ or Cs^+, is accelerated to an energy $W_p \approx 0.1$ to 0.5 MeV and guided into the plasma.

Gyro radius:

$$r_b = 1.02 \times 10^{-4} \mu^{1/2} Z^{-1} W_p^{1/2} B^{-1}$$

The primary beam is continuously ionized along its path, predominantly by collisions with plasma electrons:

$$Tl^+ + e^- \quad Tl^{++} + 2e^-$$

The secondary beam so produced has a radius half that of the primary beam (Z is doubled), so that the primary and secondary beams diverge.

An energy analyzer collects a small fraction of the secondary beam.

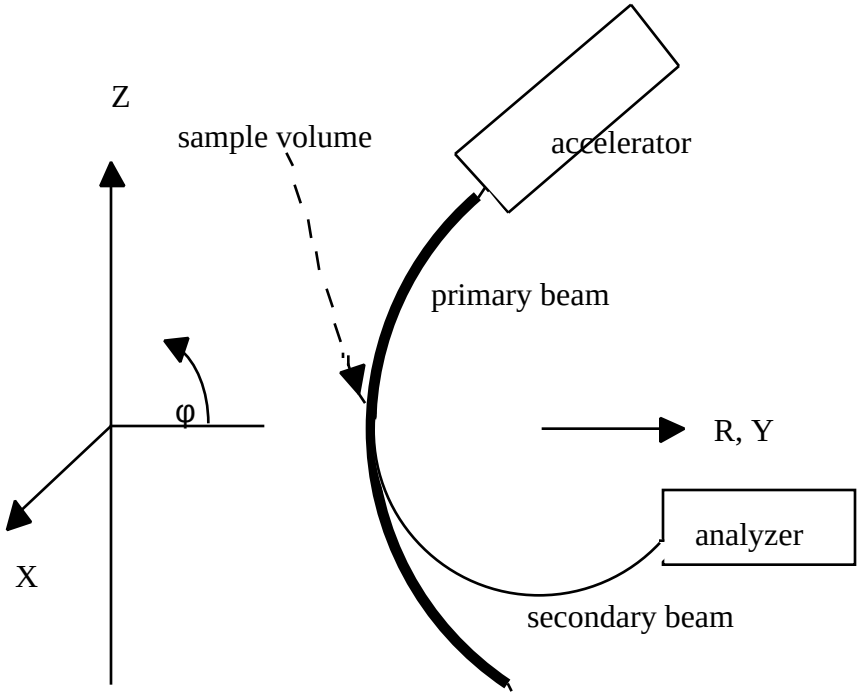

The observed secondary beam comes from a unique location within the plasma, the sample volume (sv).

The analyzer measures

the secondary beam (kinetic) energy W_S,

the position of the secondary beam on a detector plate within the analyzer, and

the secondary beam intensity.

SIMPLE VIEW OF POTENTIAL MEASUREMENTS

The electrostatic potential at the sample volume, Φ_{SV}, is measured by the difference between the secondary and primary beam energy, W_S and W_P. A primary ion with charge $q_P = Z_P e$ loses $q_P \Phi_{SV}$ of kinetic energy in reaching the sample volume. This process is path independent. The secondary ion with charge q_S gains $q_S \Phi_{SV}$ of kinetic energy between the sample volume and the energy analyzer. The analyzer measures the kinetic energy of the secondary ion,

$$W_s = W_p + \left(q_s - q_p\right)\Phi_{sv}$$

SIMPLE VIEW OF DENSITY MEASUREMENTS

The electron density n_e in the sample volume is determined from the secondary current I_S:

$$I_s = I_p n_e \delta l \sigma_{eff} \frac{q_s}{q_p}, \qquad I_p = q_p n_b v_b S$$

I_p is the primary current at the sample volume;

$$\sigma_{eff} = \frac{\langle \sigma(v_r) v_r \rangle}{v_b} \approx \frac{\langle \sigma(v_e) v_e \rangle}{v_b}$$

$\sigma(v_r)$ is cross section for electron impact ionization, $v_r = |\mathbf{v}_b - \mathbf{v}_e| \approx v_e$ is relative speed between beam ions (v_b) and plasma electrons (v_e), <...> means averaging over plasma electron energy distribution, S is beam cross sectional area, δl is sample volume length, n_b is beam density

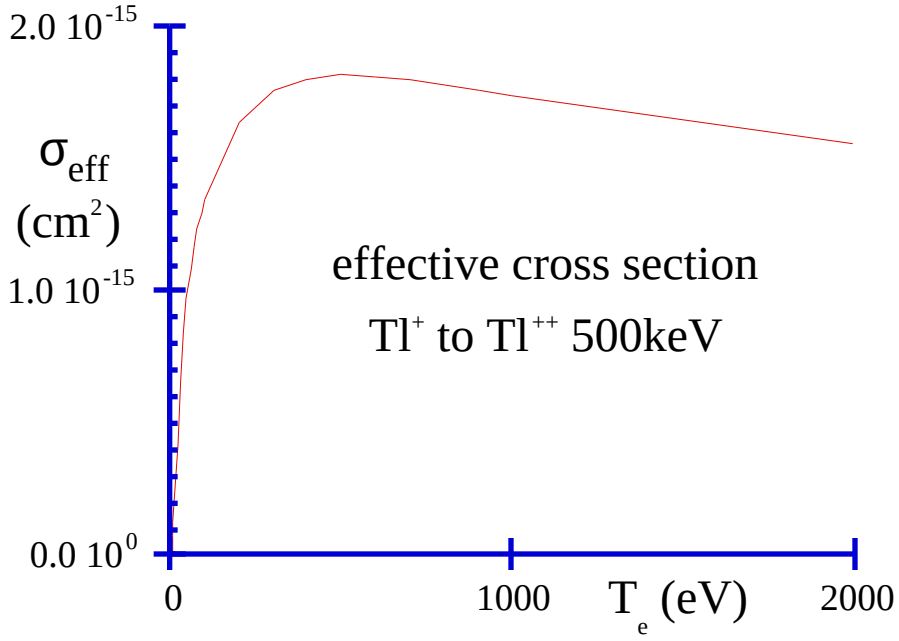

Measure a detector current I_d I_s:

$$\frac{\tilde{I}_d}{I_d} = \frac{\tilde{I}_s}{I_s} = \frac{\tilde{n}_e}{n_e}$$

SIMPLE VIEW OF MAGNETIC MEASUREMENTS

The primary beam is injected approximately in the (Y, Z) plane. For a tokamak the dominant beam bending is also in the plane (Y, Z), determined by the toroidal field B_φ. However there is also beam bending in the plane (X, Y) due to poloidal fields. Therefore by measuring the beam displacement in the toroidal or X direction information on poloidal fields, produced by toroidal currents, is available. The fluctuating components of toroidal displacement, produced by fluctuating poloidal fields, are easiest to measure.

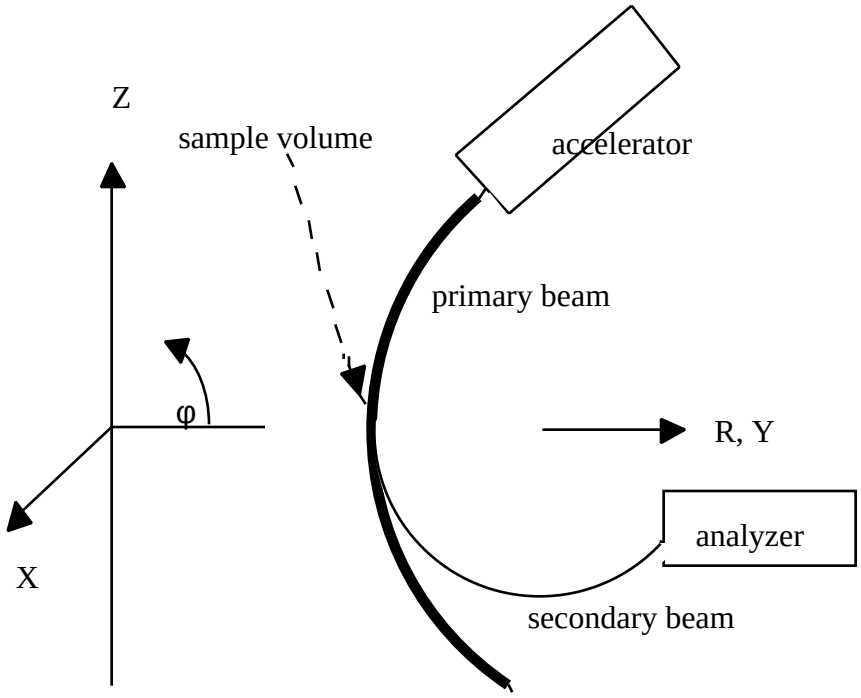

APPARATUS

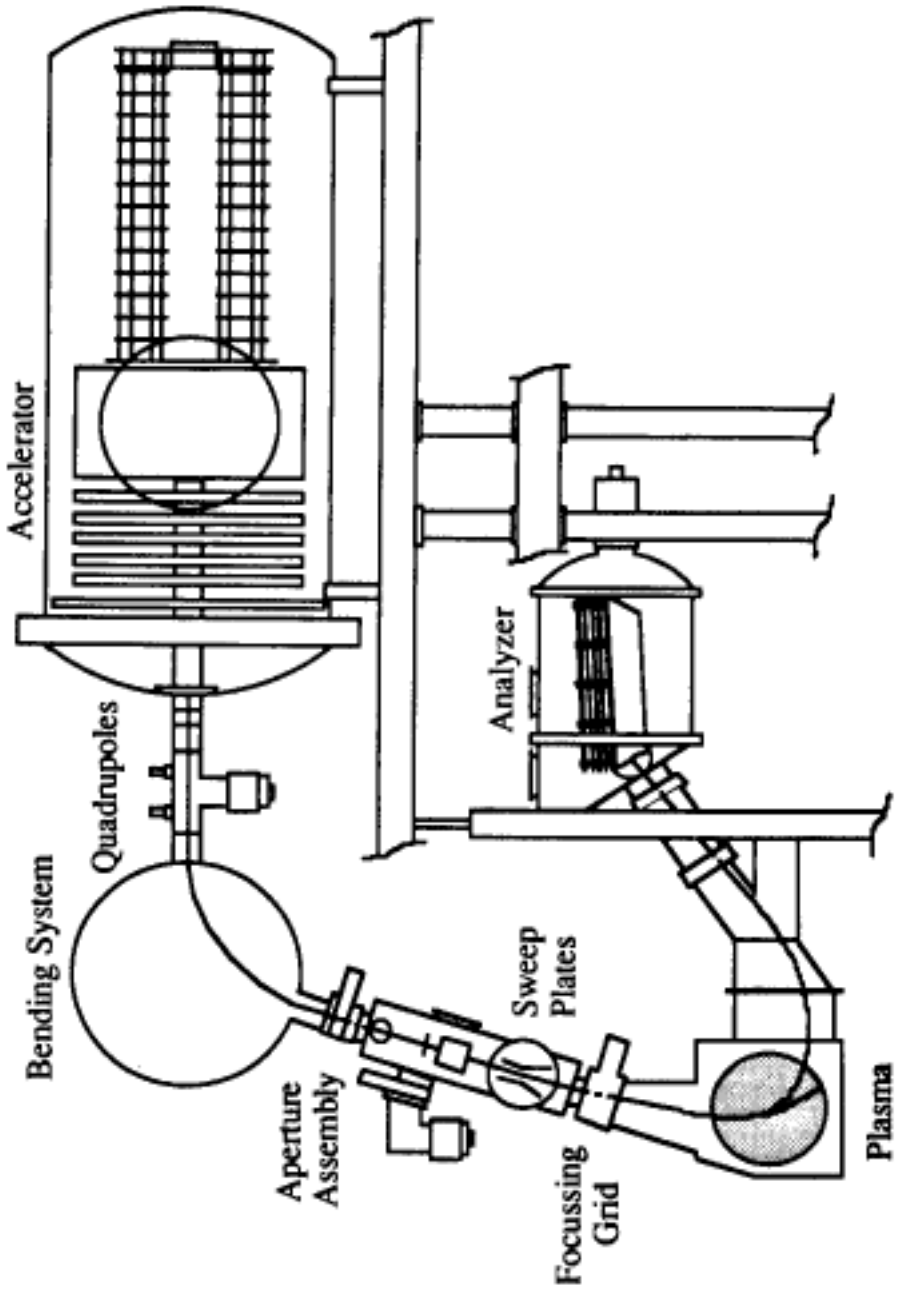
Accelerator
Quadrupoles
Bending System
Analyzer
Sweep Plates
Aperture Assembly
Focussing Grid
Plasma

The ion source. Heat Tl (202.97 and 204.97 amu) or Cs (133) loaded zeolite. Future developments: plasma sources

The accelerator . The thermal ions are extracted, focused and accelerated. Typically a Gaussian intensity profile with radius 0.2to 1cm, and a current $I_{p0} \leq 200\ \mu A$.

A 5 MeV accelerator would allow beam probing of TFTR.

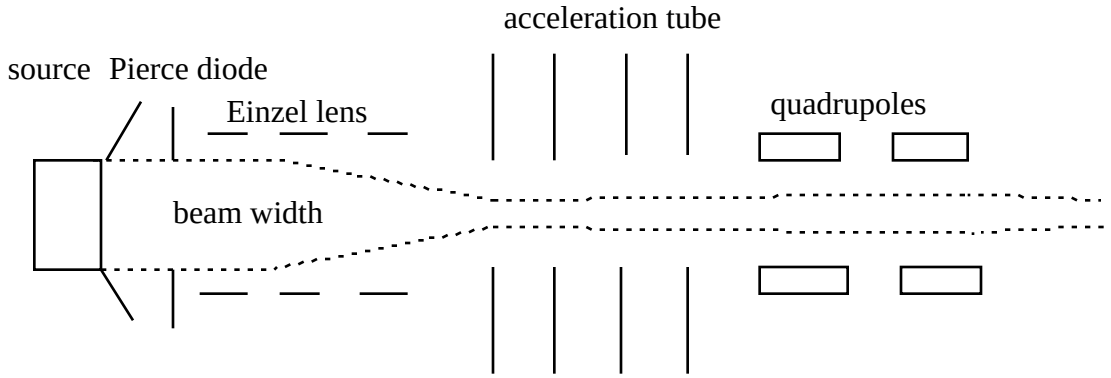

Beam bending system. Electrostatic bending systems are used to direct the beam into the plasma.

Sweep plates. Electrostatic deflection plates can be included in the primary beam line to sweep the primary beam in the (Y, Z) plane (a radial sweep), and another pair to sweep in the (X, Y) plane (a toroidal sweep).

Primary beam detectors . Two planes of parallel wires; the wires in one plane are perpendicular to the wires in the second plane. The beam intensity profile is determined by scanning the beam across one wire.

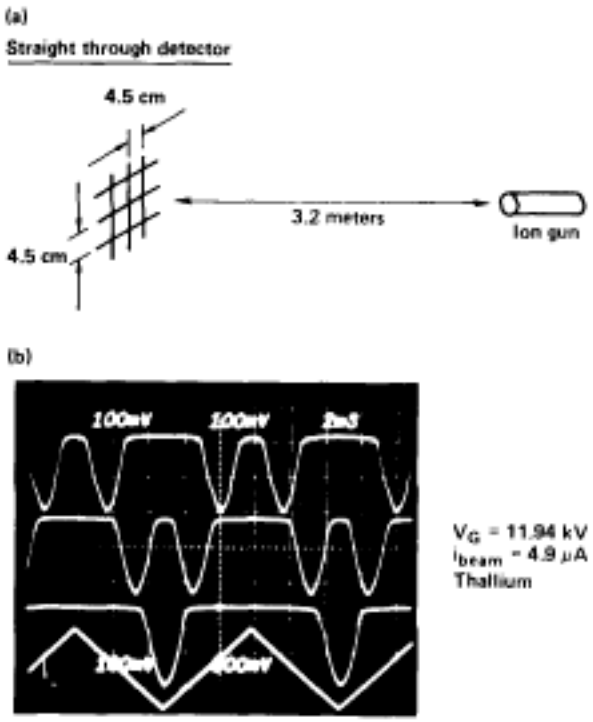

THE PARALLEL PLATE ANALYZER

A schematic showing the entrance slit, detector system, and ground plane.

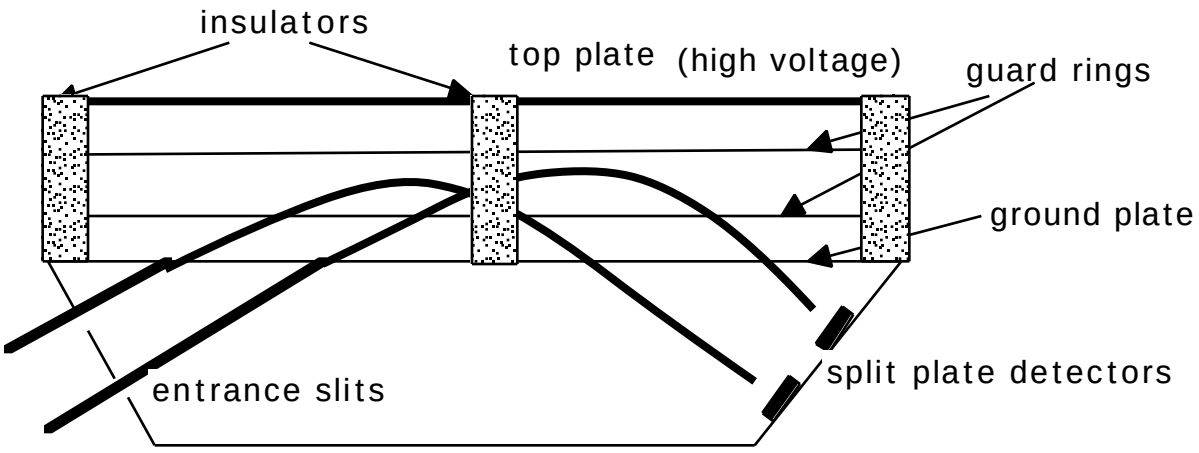

The analyzer gain G(θ) is defined by the ratio of the input secondary beam energy W_S to the voltage V_A required to center (i.e. balance) the secondary beam on the split plate detector set

$$q_s G(\theta) = \left(\frac{W_s}{W_A}\right)_{balance}$$

Then

$$\Phi_{sv} = \frac{q_s G(\theta) V_A(balance) - q_p V_p}{q_s - q_p}$$

Typical gain curve

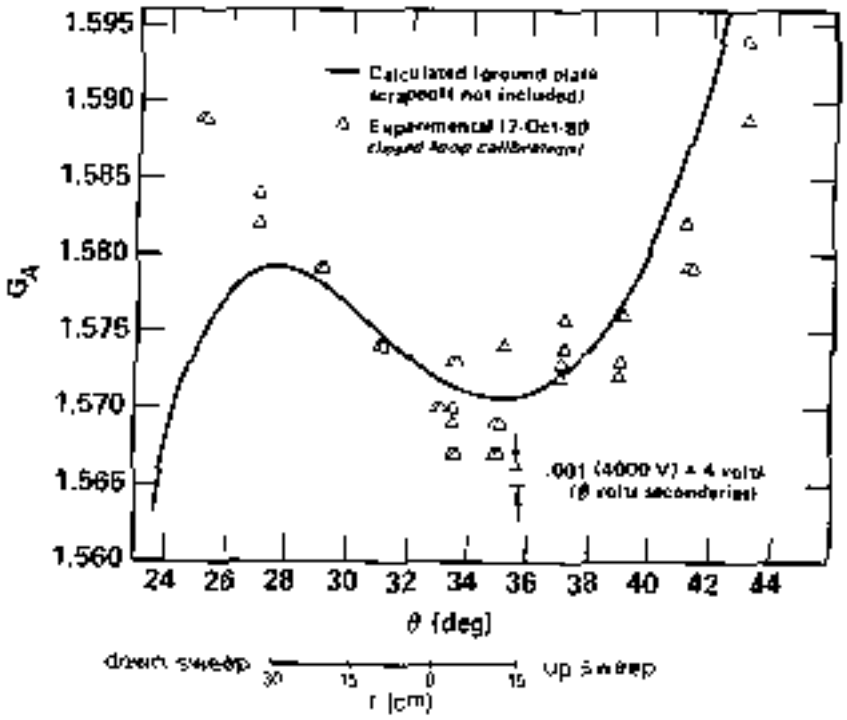

Problems: What is the entrance angle?

THE SPLIT PLATES

One split plate assembly with the finite size beam footprint. Measure $I_d = (1+\gamma_s)I_s$ with $\gamma_s \approx 3$.

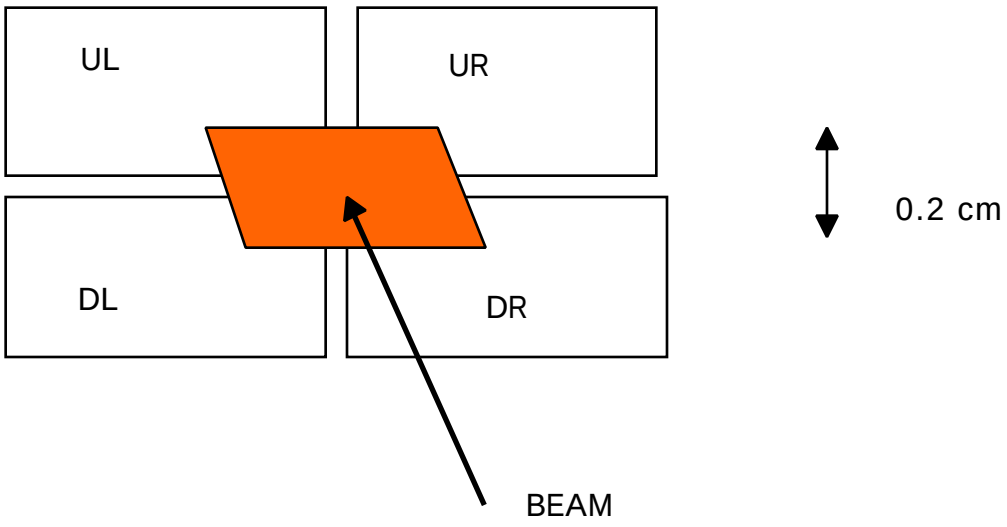

$$I_{tot} = I_{UL}+I_{DL}+I_{UR}+I_{DR}$$

$$\Delta_{LR} = [(I_{UL}+I_{DL})-(I_{UR}+I_{DR})]/I_{tot}$$

$$\Delta_{UD} = [(I_{UL}+I_{UR})-(I_{DL}+I_{DR})]/I_{tot}$$

Basic measurement	Combination	
Physics		
intensity	I_{tot}	n
intensity fluctuations:	$\tilde{I}_{tot} / I_{tot}$	$\tilde{n} / n$
up/down	Δ_{UD}	Φ
up/down fluctuations:	$\tilde{\Delta}_{UD}$	$\tilde{\Phi}$
left/right:	Δ_{LR}	$\mathbf{B}_\theta$
left/right fluctuations:	$\tilde{\Delta}_{LR}$	$\tilde{\mathbf{B}}_\theta$

Problems:

Minimize ultraviolet light.

Maintain the secondary beam in the plane of the analyzer; apparent energy = $W_S \cos^2(\alpha)$.

Maintain electric field correctly

SAMPLE VOLUMES

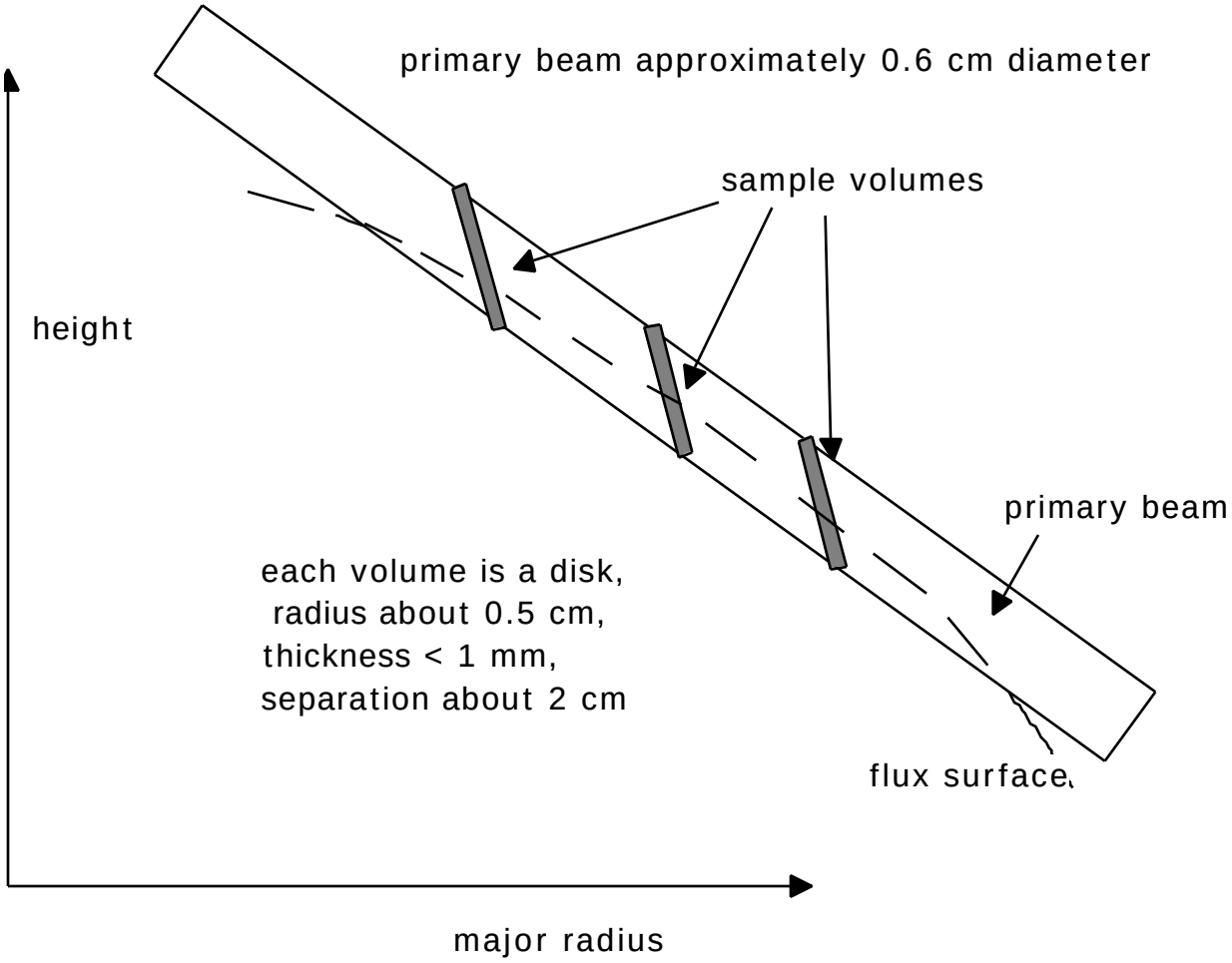

A detection grid.

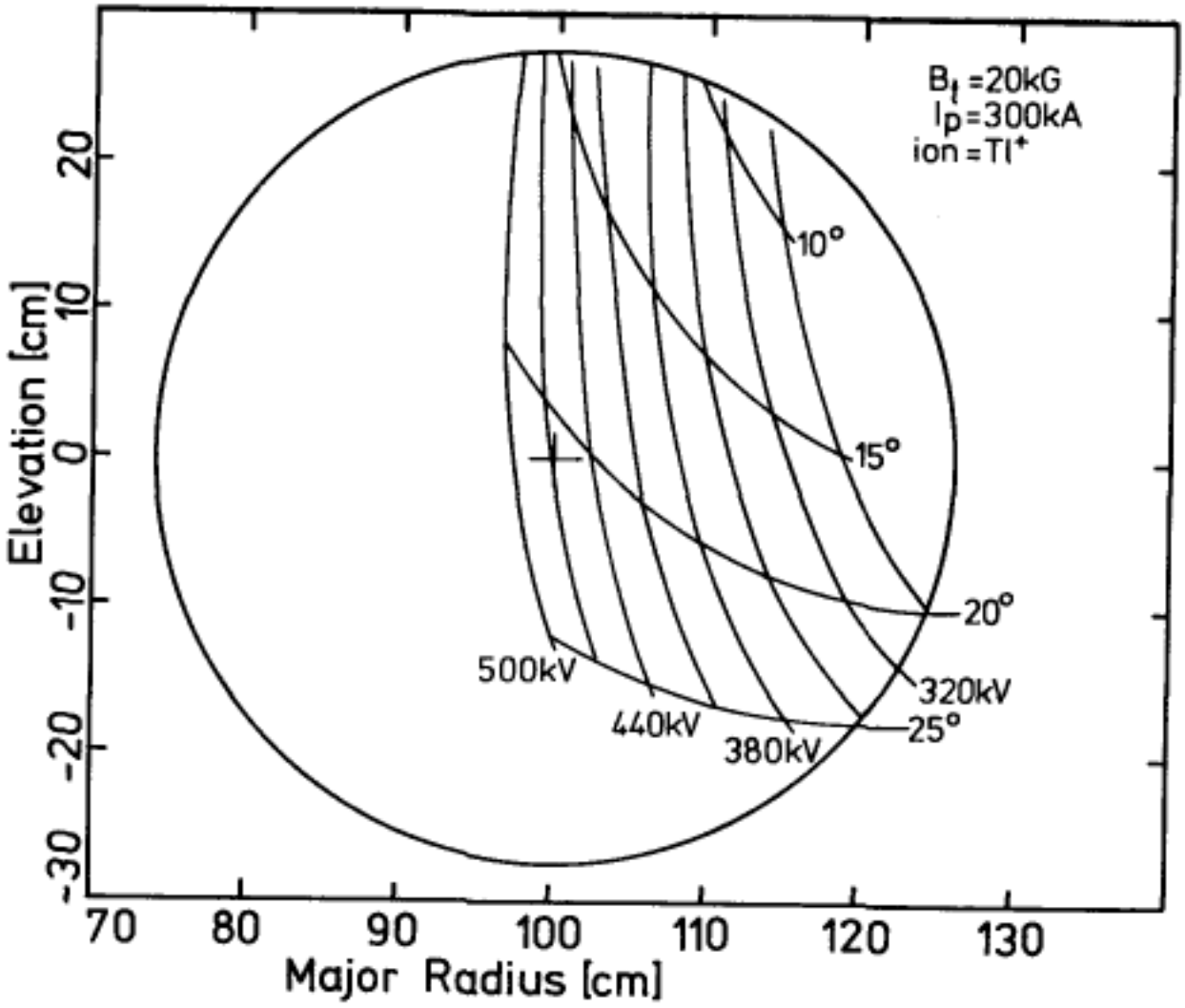

Adjacent sample volumes.

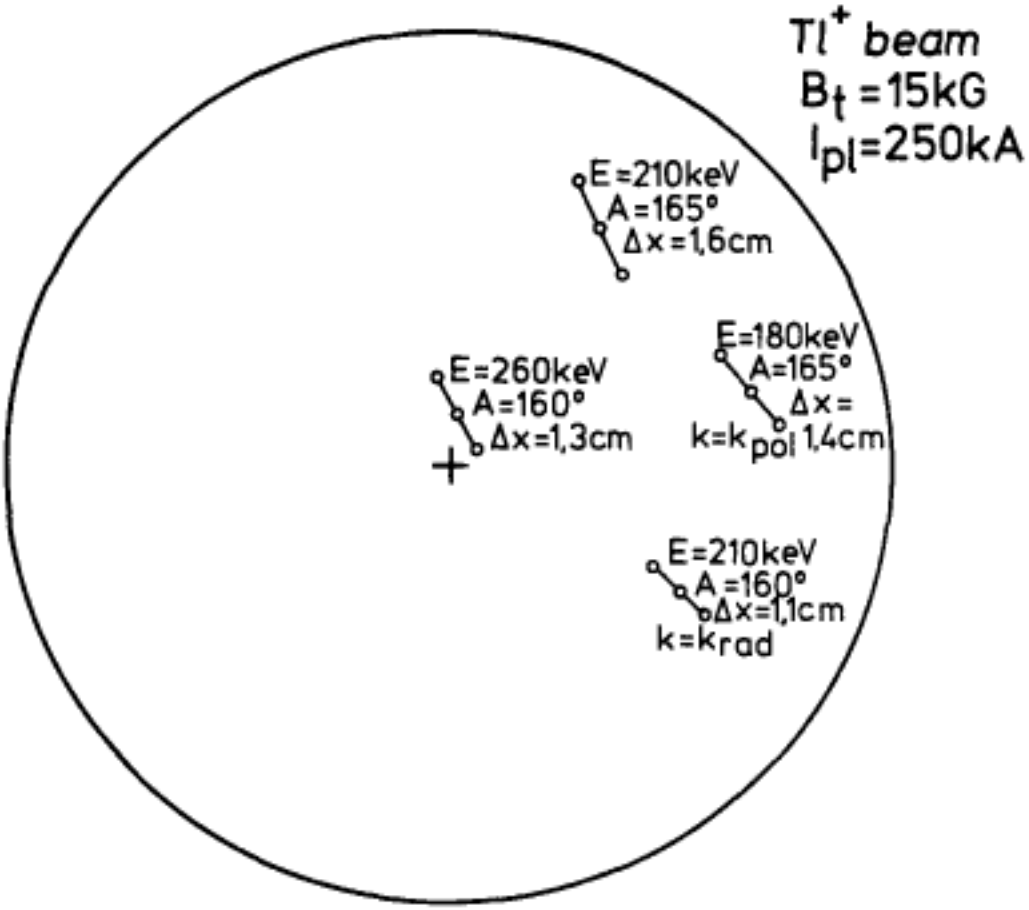

SPACE POTENTIAL , MORE DETAILS

Trajectory through plasma

$$Work = \int_a^b \boldsymbol{F} \cdot d\boldsymbol{l} = q \int_a^b \boldsymbol{E} \cdot d\boldsymbol{l}$$

$$= -q \int_a^b \nabla \Phi \cdot d\boldsymbol{l} = -q \int_a^b d\Phi = -q\left(\Phi_b - \Phi_a\right)$$

May not be purely electrostatic:

$$E = -\nabla \Phi - \frac{\partial A}{\partial t}$$

Change in energy ΔW measured by the analyzer, with $q_p = e$ and $q_s = 2e$, is

$$\Delta W = e\Phi_{sv} - e \int_a^{sv} \frac{\partial \boldsymbol{A}}{\partial t} \cdot d\boldsymbol{l} - 2e \int_{sv}^b \frac{\partial \boldsymbol{A}}{\partial t} \cdot d\boldsymbol{l}$$

Primary and secondary beams are almost in the poloidal plane (Y, Z), so only the time variation of the poloidal and radial components of A matter-generally very small.

If the primary beam is allowed to pass directly into the analyzer, then any measured energy change comes only from the time derivatives of the vector potential.

POTENTIAL PROFILES

$$\Phi_{sv}\left(q_s - q_p\right) = \frac{q_s V_A\left[G(\theta) - f(\theta)\Delta_{UD}\right]}{\cos^2(\alpha)} - q_p V_p$$

i.e. fix V_A and monitor Δ_{UD}.

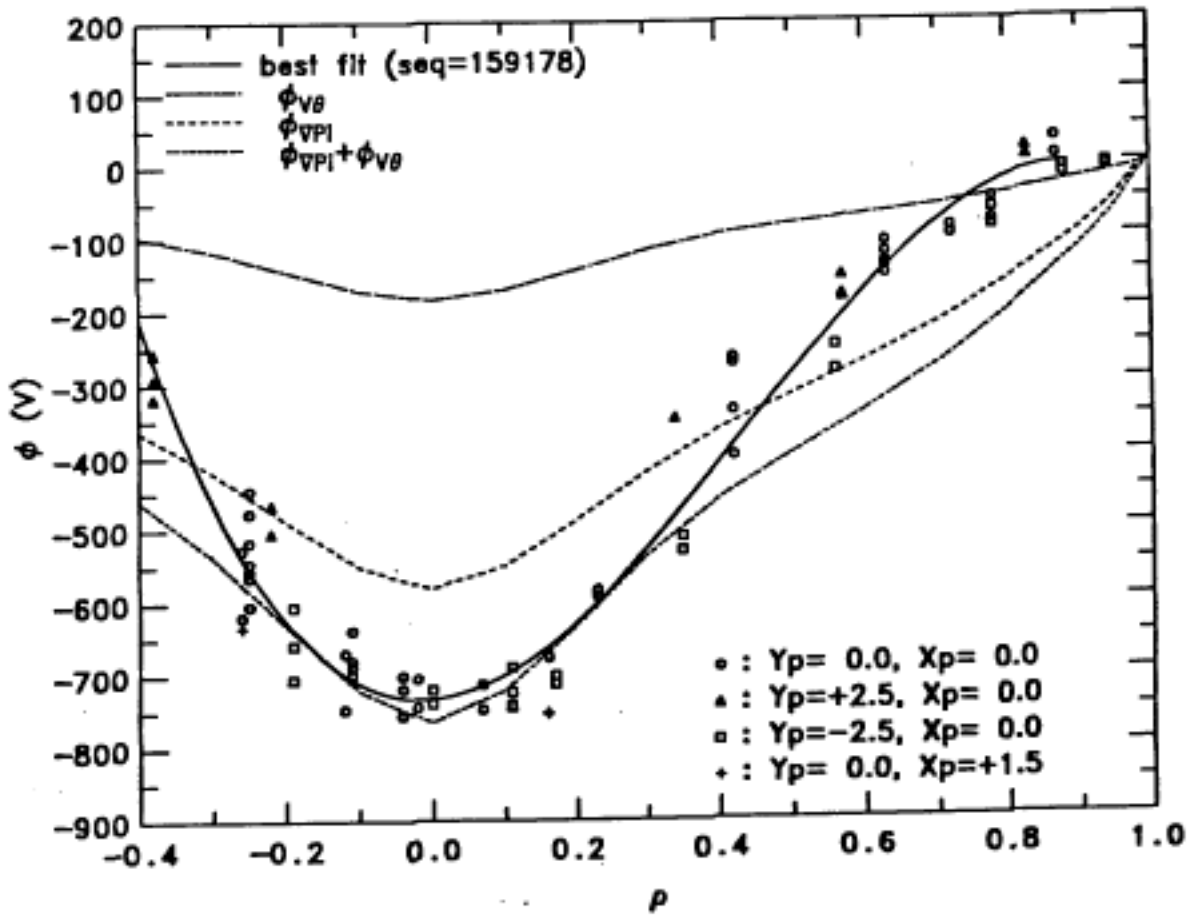

A potential profile obtained in TEXT.

Only relative values of Φ_{SV} are determined.

SPACE POTENTIAL FLUCTUATIONS

The signal Δ_{UD} fluctuates.

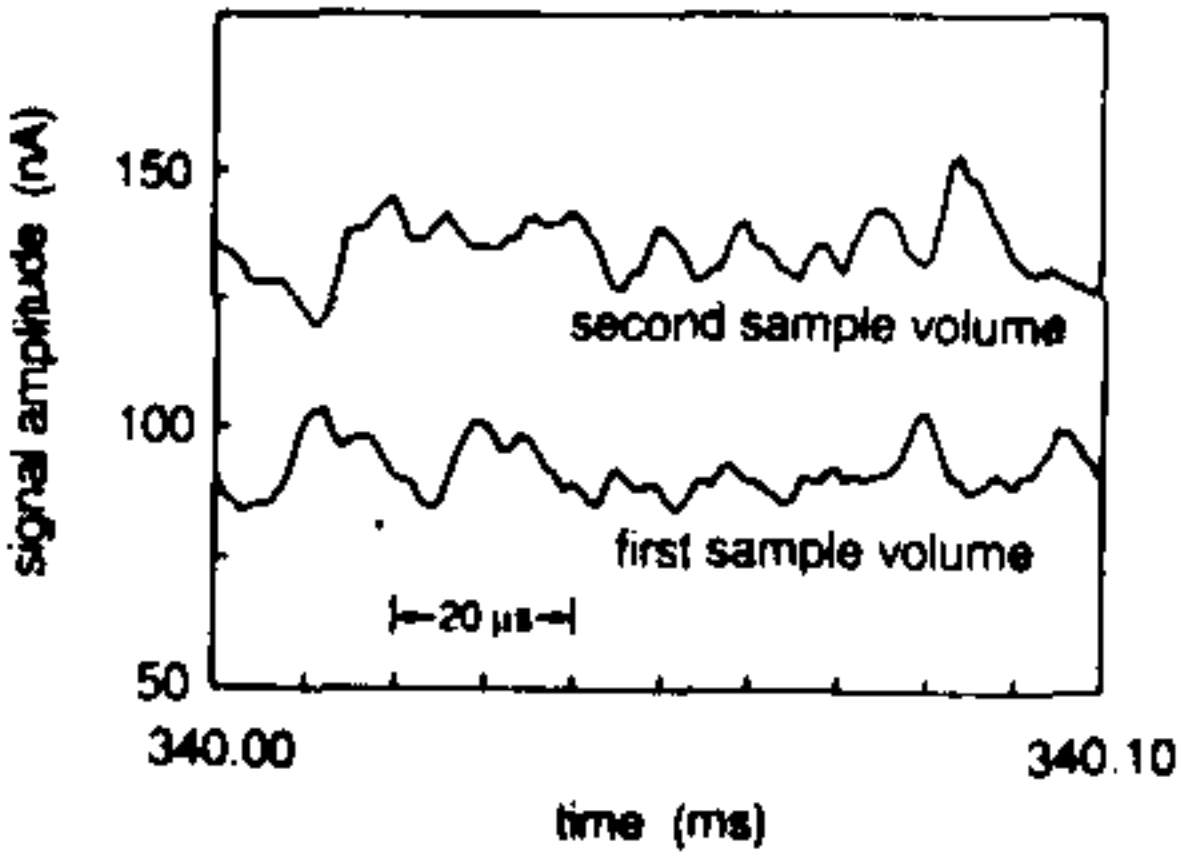

Figure 12. Time histories of potential fluctuations in two sample volumes separated poloidally by 2.3cm at a radial location r/a = 0.96 on TEXT.

'Cross talk' will appear for fluctuation wavelengths small enough such that density variations exist across the small dimension of the sample volume.

IS IT ELECTROSTATIC?

$$\nabla^2 \boldsymbol{A} = -\mu_0 \boldsymbol{j} = \frac{\mu_0}{\eta}\left(\nabla\Phi + \frac{\partial \boldsymbol{A}}{\partial t}\right)$$

For the parallel fluctuating component of A we have

$$\nabla^2 \tilde{A}_{\|} = -\mu_0 \tilde{j}_{\|} = \frac{\mu_0}{\eta}\left(\nabla_{\|}\tilde{\Phi} - i\omega\tilde{A}_{\|}\right)$$

The electrostatic limit corresponds to

$$\nabla_{\|}\tilde{\Phi} >> i\omega\tilde{A}_{\|} \qquad \text{or} \quad k^2 >> \frac{\mu_0\omega}{\eta}$$

Any fluctuating Δ_{UD} observed on primary is from time varying magnetic fields ONLY.

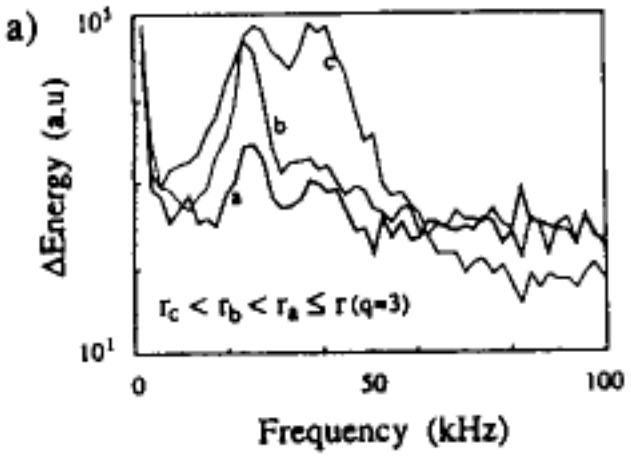

secondaries

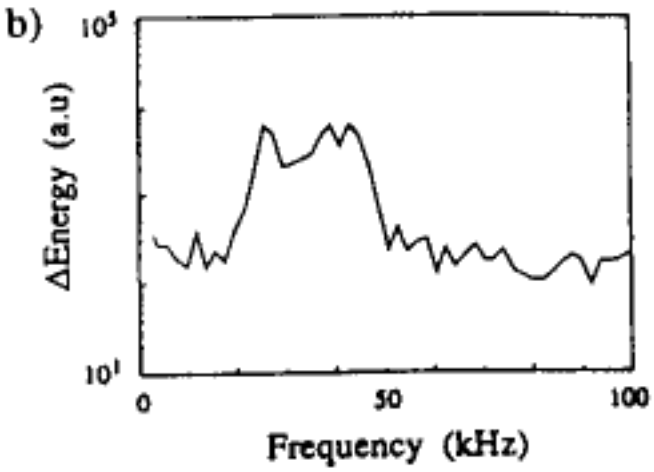

primary

The prominent feature between 20 and 50 kHz is electromagnetic

DENSITY FLUCTUATIONS

The secondary current at the detector is

$$I_{sd} = 2 I_{p0} \exp\left[-\int_0^{sv} n_e \sigma^{\Sigma}_{eff,1} dl_1\right] \left(n_e \sigma_{eff,1,2} dl\right) \exp\left[-\int_{sv}^{R} n_e \sigma^{\Sigma}_{eff,2} dl_2\right]$$

where

$$\sigma^{\Sigma}_{eff,\alpha} = \sum_{\beta>\alpha} \sigma_{eff,\alpha,\beta}$$

For small fluctuation amplitudes:

$$\frac{\tilde{I}_{tot}}{I_{tot}} = \frac{\tilde{I}_{s,d}}{I_{s,d}} = \frac{\tilde{n}_e(sv)}{n_e(sv)} - \int_0^{sv} \tilde{n}_e \sigma^{\Sigma}_{eff,1} dl_1 - \int_{sv}^{R} \tilde{n}_e \sigma^{\Sigma}_{eff,2} dl_2$$

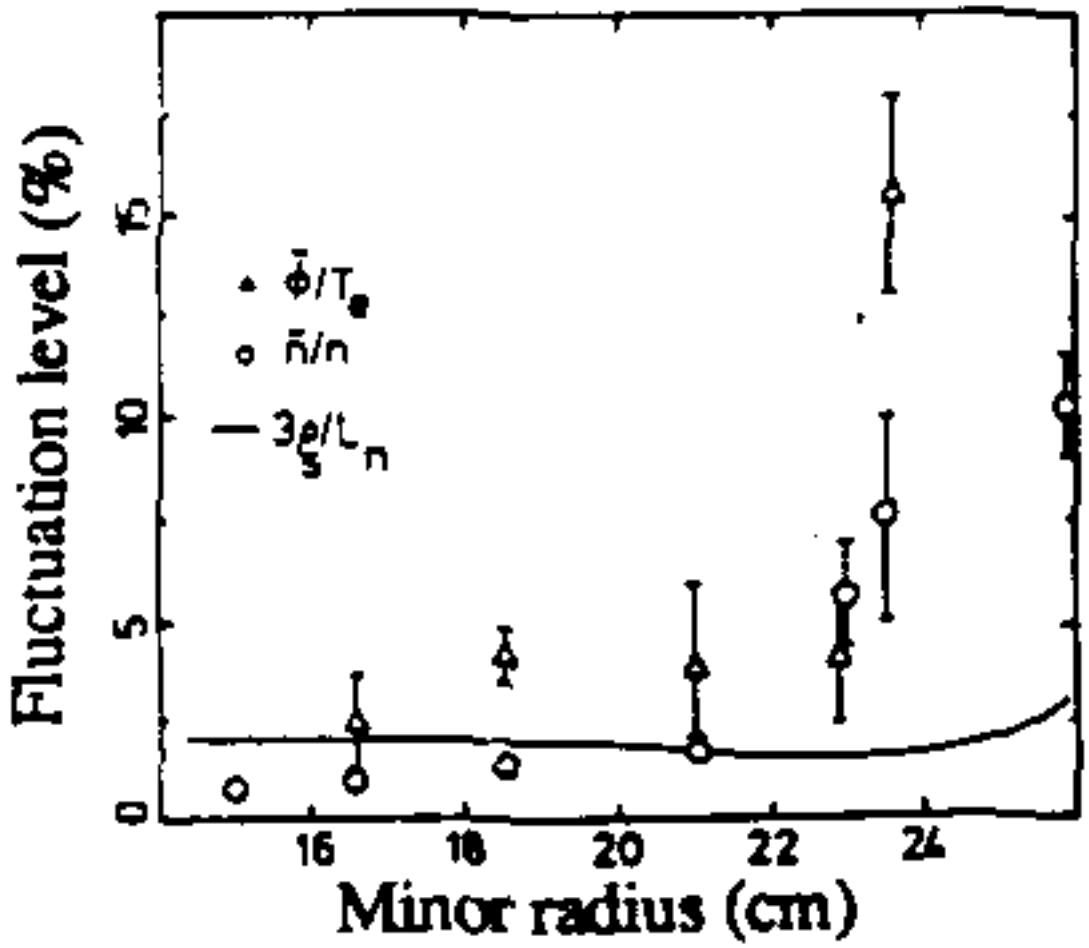

Profiles of $\left(\tilde{n}_e / n_e\right)_{rms}$ (circles) and $\left(\tilde{\phi} / T_e\right)_{rms}$ (triangles) in TEXT

TWO-POINT MEASUREMENTS

$$\bar{P}_\omega(r_1, r_2) = \bar{S}_\omega \bar{\gamma}_\omega(r_1, r_2) e^{i\bar{\varphi}_\omega(r_1, r_2)}$$

$$\bar{S}_\omega = \left[|\bar{P}_\omega(r_1, r_1)| |\bar{P}_\omega(r_2, r_2)| \right]^{\frac{1}{2}}$$

$$\bar{\gamma}_\omega(r_1, r_2) = \frac{\bar{P}_\omega(r_1, r_2)}{|\bar{P}_\omega(r_1)|^{1/2} |\bar{P}_\omega(r_2)|^{1/2}}$$

$$\bar{\varphi}_\omega(r_1, r_2) = \arg \bar{P}_\omega(r_1, r_2)$$

This allows the average wave number k_ω to be calculated:

$$\bar{k}_\omega(r_1, r_2) = \frac{\bar{\varphi}_\omega(r_1, r_2)}{|r_1 - r_2|}$$

$$\bar{k}_\omega(r_1, r_2) = \frac{\bar{\varphi}_\omega(r_1, r_2)}{|r_1 - r_2|}$$

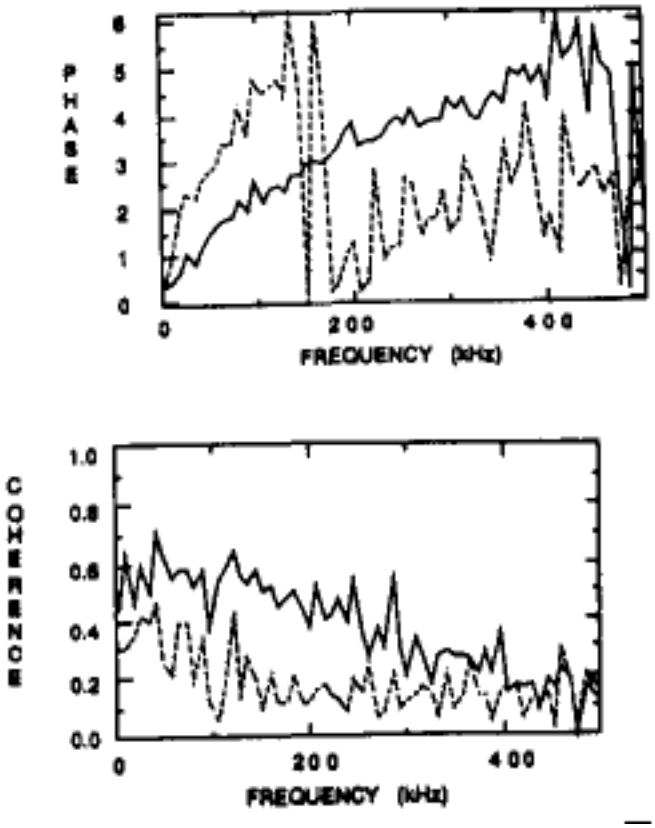

Phase and coherence. Sample volumes poloidally separated by d = 2.4 cm (solid line) and 4.7 cm (broken line) at r/a ≈ 0.75.

$\bar{\varphi}_\omega$ is smoothly varying with f = ω/2π for the 2.4 cm separation, so that $\bar{k}$ is unambiguous.

$v_{ph} = \omega/k(\omega)$ is about 6×10^5 cms^{-1}.

$\gamma = \exp(-d/l_c)^2)$, and $l_c \approx 4$ cm.

THE PARTICLE FLUX

$$\Gamma_r = \langle \tilde{n}\tilde{v}_r \rangle = \frac{\langle \tilde{n}(t)\tilde{E}_r(t) \rangle}{B}$$

$$\Gamma_r = \frac{2}{B}\int_0^\infty \mathrm{Re}\left[P_{\tilde{n}\tilde{E}}(\omega) d\omega \right]$$

$$= \frac{1}{B}\int_0^\infty \tilde{n}_{rms}\tilde{\Phi}_{rms}(\omega) k_\theta(\omega) |\gamma_{\tilde{n}\tilde{\Phi}}(\omega)| \sin\left(\alpha_{\tilde{n}\tilde{\Phi}}(\omega)\right) d\omega$$

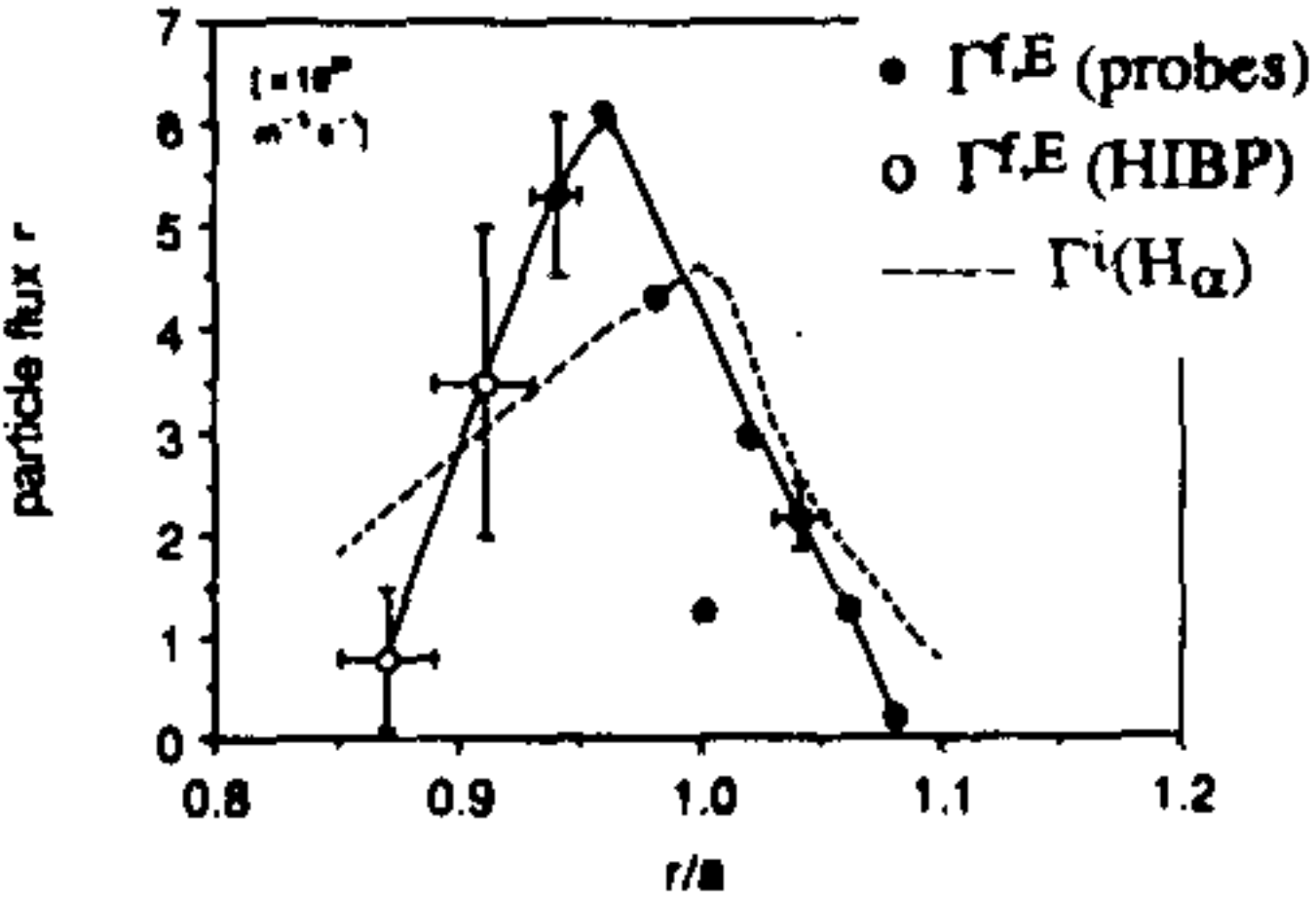

Electrostatic turbulence driven particle flux from HIBP and probes, and the total particle flux $\Gamma^i(H\alpha)$ from spectroscopy.

LINE-INTEGRAL EFFECTS

1) Beam attenuation limits the HIBP's ability to probe the center of the machine.

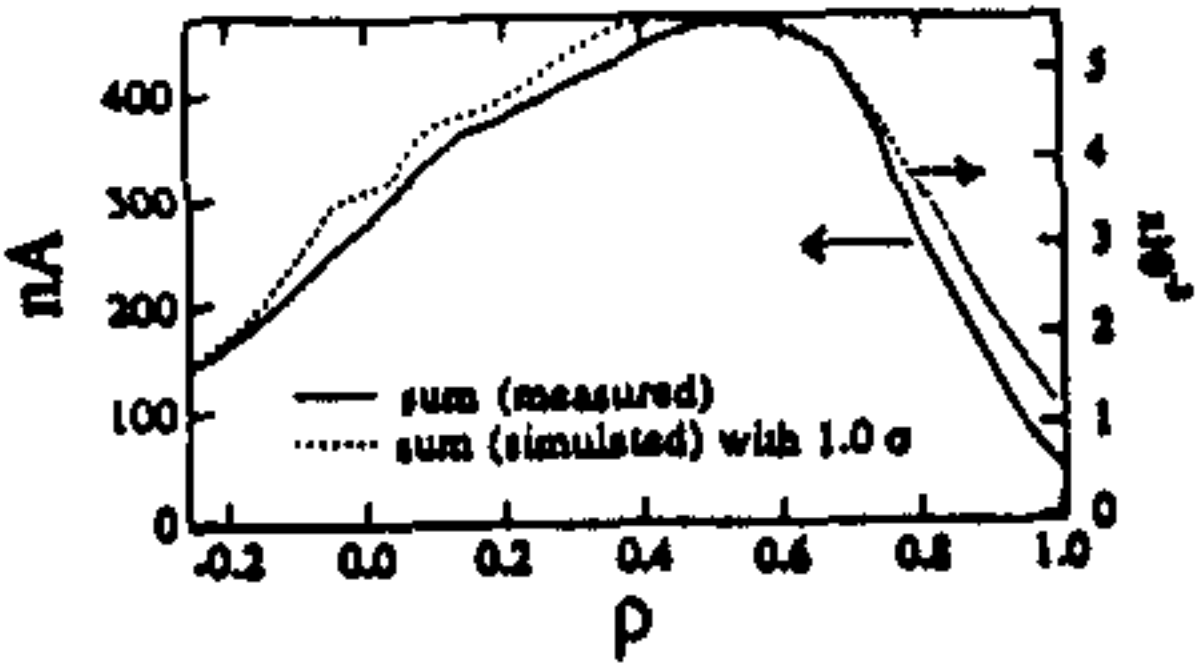

The experimentally measured sum signal I_{tot} (solid line) in nA and the simulated secondary current (broken line) as a fraction of the primary beam current.

2) Fluctuations along primary and secondary beam corrupts measurement of $\tilde{n}$. Two key dimensionless factors, $n_e \sigma_{eff} L \approx 1$ and $l_c/L << 1$. Higher densities or cross sections (more beam attenuation), or smaller values of kl_c, are worse. For $\bar{n} > 4 \times 10^{19}$ m^{-3} in TEXT these effects should appear. Higher V_A implies smaller σ_{eff}, and smaller effects.

FINITE SAMPLE-VOLUME EFFECTS

There are three important effects to consider:

filtering of higher wave numbers,

reducing apparent phase, and

increasing apparent coherence.

All three have been quantified using a model for the turbulence based on Gaussian statistics. They are negligible as long as $b < l_C$ and $b < 1/\bar{k}$, where 2b is the sample volume dimension, l_C the correlation length and $\bar{k}$ an average wave number along b.

MAGNETIC FIELD MEASUREMENTS

Toroidal or left-right (LR) motion Δ_{LR} of the secondary beam across the detector plates gives information on poloidal fields.

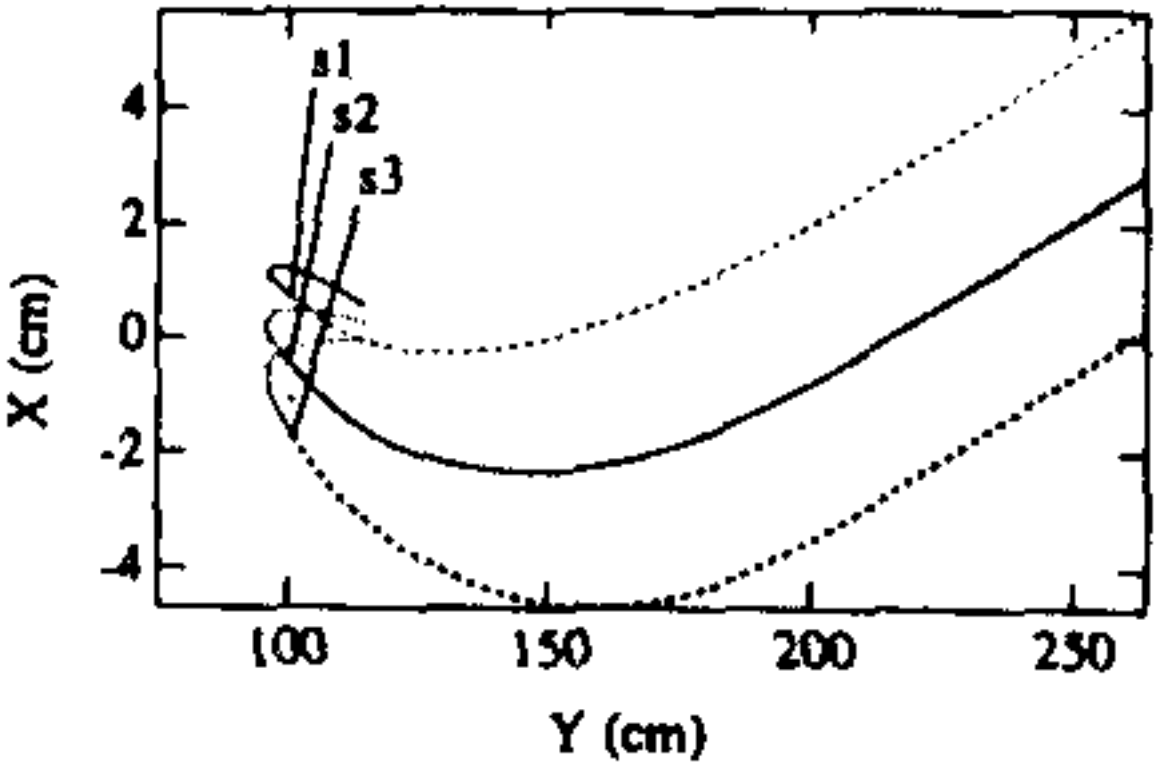

Computed primary and secondary beam trajectories, projected in the horizontal plane, for three different toroidal steering angles. The fields include a rippled toroidal field (i.e. not toroidally symmetric), together with plasma equilibrium fields.

MAGNETIC FLUCTUATIONS IN TOROIDAL SYMMETRY

Toroidal component of canonical momentum of charged particle with mass m, toroidal velocity v_φ, is conserved:

$$P_\varphi = mRv_\varphi + qRA_\varphi = \text{constant}$$

Apply to the primary beam between the source (subscript 0) and the ionization point (subscript i) in the sample volume:

$$mR_0 v_{\varphi 0} + eR_0 A_{\varphi 0} = mR_i v_{\varphi i} + eR_i A_{\varphi i}$$

Apply to the secondary ion between the ionization point and the detector (subscript d):

$$mR_i v_{\varphi i} + 2eR_i A_{\varphi i} = mR_d v_{\varphi d} + 2eR_d A_{\varphi d}$$

At ionization point the primary and secondary ions have the same value of v_φ. Therefore

$$A_{\varphi i} = \frac{m}{e}\left(\frac{R_d}{R_i} v_{\varphi d} - \frac{R_0}{R_i} v_{\varphi 0}\right) + 2\frac{R_d}{R_i} A_{\varphi d} - \frac{R_0}{R_i} A_{\varphi 0}$$

i.e. the toroidal velocity of the secondary ion at the detector $v_{\varphi d}$ carries information about the vector potential $A_{\varphi i}$ at the sample volume, if the system is toroidally symmetric. Considering fluctuations which decay rapidly in space, so that $\tilde{A}_{\varphi 0} = \tilde{A}_{\varphi d} = 0$,

$$\tilde{A}_{\varphi i} = \frac{m}{e}\left(\frac{R_d}{R_i} \tilde{v}_{\varphi d}\right)$$

Problems

1) we do not measure $\tilde{v}_{\varphi d}$, but rather $\tilde{\Delta}_{LR}$.

2) the tokamak fields are not axisymmetric.

Therefore use "toroidal symmetry" result for A_φ as a first iteration in a particle trajectory simulation to predict displacement at detector. Iterate assumed A_φ until measured and computed displacement agree.